Paleoceanography and Paleoclimatology

RESEARCH ARTICLE
10.1029/2020PA003924

Special Section:
The Miocene: The Future of the Past

Temperature Gradients Across the Pacific Ocean During the Middle Miocene

Lyndsey R. Fox[1,2], Bridget S. Wade[1,3], Ann Holbourn[4], Melanie J. Leng[5,6], and Rehemat Bhatia[3]

[1]School of Earth and Environment, University of Leeds, Leeds, UK, [2]School of Engineering and Environment, Kingston University, Surrey, UK, [3]Department of Earth Sciences, University College London, London, UK, [4]Institute of Geosciences, Christian-Albrechts-University, Kiel, Germany, [5]National Environmental Isotope Facility, British Geological Survey, Nottingham, UK, [6]School of Biosciences, University of Nottingham, Sutton Bonington Campus, Nr Loughborough, UK

Abstract Sea surface temperatures (SSTs) of the tropical Pacific Ocean exert powerful controls on regional and global climates. Previous studies have suggested that during warm climate phases, the east-west temperature gradient collapsed. To date, there has been no high-resolution reconstruction of sea surface conditions in both the east and west Pacific Ocean during the Miocene Climate Optimum (MCO) and across the middle Miocene climate transition (MMCT); therefore, our understanding of the mean oceanographic state during this major global climatic shift is limited. Here, we present new SST reconstructions for the eastern Pacific Ocean (15.5–13.3 Ma) which show a clear east-west temperature gradient of ~4°C during the warmest interval of the Neogene, implying that the oceanographic processes that produce the modern gradient were present and active. There is no shift in the east-west gradient across the MMCT indicating that the gradient was not impacted by global cooling and ice growth. We find a 2°C sea surface cooling in the eastern equatorial Pacific, that lags the benthic foraminiferal $\delta^{18}O$ positive shift by 150 kyr, indicating that tropical temperature did not decrease synchronously with the expansion of the Antarctic ice sheet. Reconstructed variations in the $\delta^{18}O$ composition of seawater, determined by combining our Mg/Ca and $\delta^{18}O$ records, reveal a freshening in the eastern Pacific Ocean after 13.8 Ma, suggesting changes in the hydrological cycle and in tropical fronts in response to the new icehouse regime.

Plain Language Summary In the modern ocean, there is a large temperature gradient between the western and eastern tropical Pacific Ocean due to the contrast between the West Pacific Warm Pool waters and cold upwelling waters in the east. We used the geochemistry of fossil microorganisms sampled from a sediment core to reconstruct sea surface temperatures during an interval of the Earth's history (15.5–13.3 million years ago) that was warmer than today. Our results indicate that during the warmest climate phase of the last 23 million years, there was still a temperature gradient between the western and eastern Pacific and this gradient continued throughout a subsequent interval of climate cooling.

Key Points:

- High resolution foraminiferal $\delta^{18}O$ coupled with Mg/Ca, provide detail on temperature and $\delta^{18}O$ composition of seawater between 15.5 and 13.3 Ma
- Miocene SST records reveal an E-W gradient of ~4°C across the Pacific, which remained constant through an interval of ice sheet expansion
- Surface water freshening post 13.8 Ma suggests changes to the hydrological cycle/tropical fronts due to enhanced meridional thermal gradients

Correspondence to:
L. R. Fox,
l.fox@kingston.ac.uk

Citation:
Fox, L. R., Wade, B. S., Holbourn, A., Leng, M. J., & Bhatia, R. (2021). Temperature gradients across the Pacific Ocean during the middle Miocene. *Paleoceanography and Paleoclimatology*, *36*, e2020PA003924. https://doi.org/10.1029/2020PA003924

Received 19 MAR 2020
Accepted 20 MAY 2021

Author Contributions:
Conceptualization: Lyndsey R. Fox, Bridget S. Wade, Ann Holbourn
Data curation: Lyndsey R. Fox
Formal analysis: Lyndsey R. Fox
Funding acquisition: Bridget S. Wade, Ann Holbourn
Investigation: Lyndsey R. Fox, Bridget S. Wade, Ann Holbourn
Methodology: Lyndsey R. Fox, Bridget S. Wade, Ann Holbourn, Rehemat Bhatia
Project Administration: Lyndsey R. Fox, Bridget S. Wade

1. Introduction

The Pacific Ocean is a key component of the global climate system as it represents the world's largest oceanic source of water vapor and CO_2 to the atmosphere, and substantially influences global atmospheric circulation patterns (Lea et al., 2000). Today, surface water conditions in the tropical Pacific Ocean are characterized by a strong east-west (E-W) gradient in sea surface temperatures (SSTs) (~4°C–5°C offset) and in thermocline depth (~50 m in the Eastern Equatorial Pacific (EEP) vs. >150 m in the Western Equatorial Pacific), with a tight coupling of the thermocline and nutricline (Lea et al., 2000; Nathan & Leckie, 2009). The formation of the modern circulation system in the tropical Pacific Ocean is believed to have developed at around ~12 Ma in response to the tectonic constriction of the Indonesian and Central American seaways. These events resulted in the restriction of Indonesian Throughflow and the development of a "proto-warm pool" in the west Pacific Ocean (Matsui et al., 2017; Nathan & Leckie, 2009), whereas trans-equatorial Pacific circulation existed prior to this (Kennett et al., 1985). Today, the West Pacific Warm Pool (WPWP) occupies much of the tropical region of the western Pacific and eastern Indian Oceans and forms a major component of the equatorial current system and El Niño-Southern Oscillation (ENSO) (Yan et al, 1992).

Resources: Bridget S. Wade, Ann Holbourn, Melanie J. Leng
Supervision: Bridget S. Wade
Visualization: Lyndsey R. Fox
Writing – original draft: Lyndsey R. Fox
Writing – review & editing: Lyndsey R. Fox, Bridget S. Wade, Ann Holbourn, Melanie J. Leng, Rehemat Bhatia

With average annual temperatures >28°C, the WPWP is the warmest water body on Earth and contributes to the heating of the tropical atmosphere, affecting both the Hadley and Walker Circulations (De Deckker, 2016; Nathan & Leckie, 2009). Investigations into the initiation of the WPWP and development of equatorial Pacific SST gradients during the middle Miocene have been hindered by a paucity of high resolution geochemical records extending beyond 13 Ma. However, Ocean Drilling Program (ODP) Site 1146 (116°16.37′E, 19°27.40′N) is located in the South China Sea (SCS) at the northern edge of the WPWP. High resolution (~3–6 k.y.) middle Miocene upper ocean temperature and salinity estimates derived from planktonic foraminiferal $\delta^{18}O$ and Mg/Ca reaching back to ~15.7 Ma were previously generated at this site (Holbourn et al., 2010).

The seasonal and decadal variability of SSTs and the extent of warm water masses in the SCS are highly correlated with the development of the WPWP, suggesting that the WPWP strongly influences surface hydrology in the SCS (e.g., Lin et al., 2011). Although seasonality is more pronounced in the SCS, in comparison to the core area of the WPWP, the summer SST signal (mainly recorded in surface dwelling planktonic foraminifera) closely tracks long-term (decadal) variability in the WPWP (Lin et al., 2011). In the middle Miocene, when the SCS was more open to the western equatorial Pacific Ocean and when polar ice sheets may have been reduced and the latitudinal temperature gradient decreased, connections between the SCS and WPWP were presumably even stronger than they are at present. This notion is also supported by a comparison of tropical SST over the past 12 Myr, which shows comparable values and trends at ODP Site 1143 (South China Sea) and at ODP Site 806 (center of WPWP) during the Miocene (Zhang et al., 2014).

The present day EEP is characterized by cold nutrient–rich waters that result from a shallow thermocline and intense upwelling. The modern SST gradient between the EEP and WPWP averages 4°C–5°C (Karnauskas et al., 2009; Figure 1) and varies in response to ENSO (Zhang et al., 2014). The absence of an equatorial temperature gradient, caused by weak trade winds and the eastward propagation of warm western Pacific equatorial waters, is thought to reflect a "permanent El-Niño" state, which results in deeper thermocline depths and attenuated upwelling rates in the EEP (Wara et al., 2005). The establishment of "permanent El-Niño" like conditions has been suggested to have taken place during intervals of global warmth, for exam-

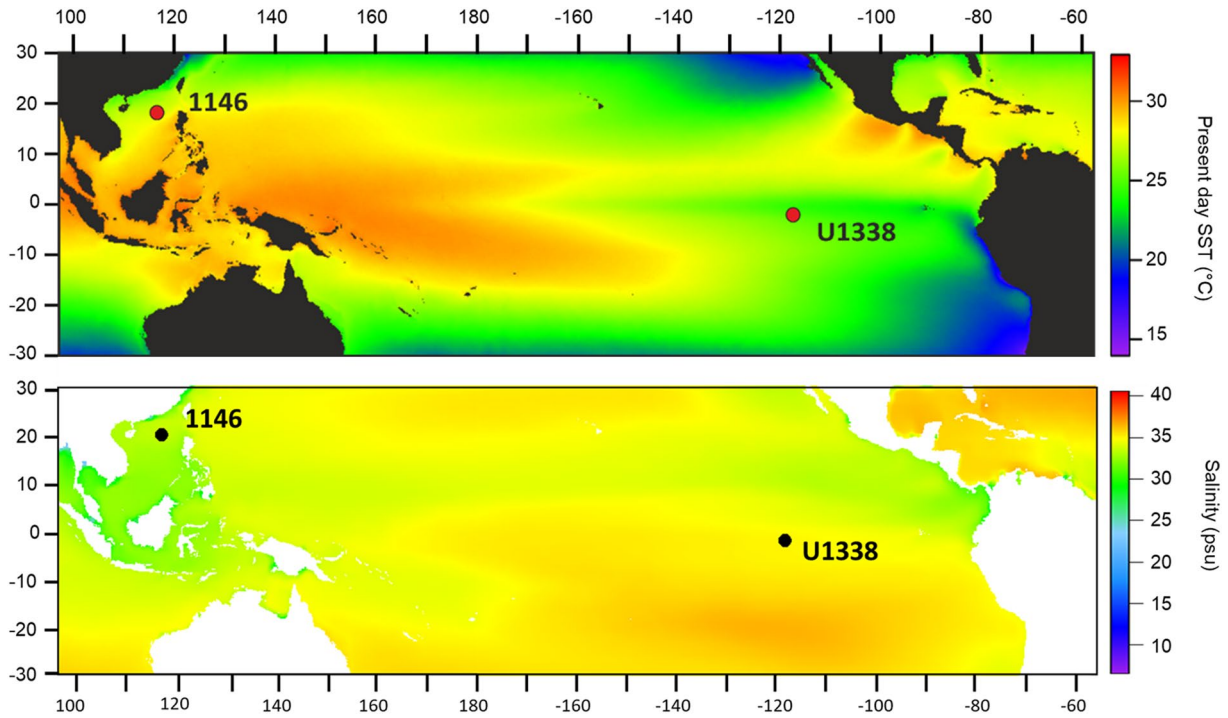

Figure 1. Paleo-location of tropical Pacific sites discussed in this study. Top panel: Colors represent remotely sensed long-term mean sea surface temperature (SST); Bottom panel: Colors represent remotely sensed long-term mean sea surface salinity (SSS) (data from Tyberghein et al. (2012), Maps were generated using the rdgal and ggplot2 packages in R.

ple during the early Pliocene when planktonic foraminiferal Mg/Ca data reveal that the E-W temperature gradient was nearly absent (Fedorov et al., 2006; Wara et al., 2005). More recently, this hypothesis has been challenged as new SST reconstructions from TEX_{86} and U^{K}_{37} revealed a sustained temperature gradient between the east and west Pacific Ocean extending back 12 million years (O'Brien et al., 2014; Zhang et al., 2014). Given the absence of high resolution geochemical records from the WPWP, we compared the planktonic foraminiferal $\delta^{18}O$ and Mg/Ca records from IODP Site U1338 (2°30.47′N, 117°58.18′W, 4200 m water depth) in the EEP with those from ODP Site 1146 (19°27.40′N, 116°16.37′E, 2092 m water depth) in the northern South China Sea (Holbourn et al., 2010; Figure 1).

Despite extensive studies of benthic foraminifera (e.g., Badger et al., 2013; Gasperi & Kennett, 1993; Holbourn et al., 2014; Shevenell et al., 2004; Tian et al., 2013) existing planktonic foraminiferal stable isotope records spanning the middle Miocene are scarce and of low resolution for the eastern equatorial Pacific Ocean. This is due to sedimentary successions spanning this interval having been strongly affected by carbonate dissolution or burial diagenesis, or proved incomplete due to hiatuses (Barron & Keller, 1982; Pearson, 1995). However, continuous sediment cores were recovered at both Site 1146 (Holbourn et al., 2010) and Site U1338, with abundant and diverse planktonic foraminifera in middle Miocene sediments (Fox & Wade, 2013). The Expedition 320/321 sites have been shown to be sensitive to dissolution (Kochhann et al., 2016), which could alter our Mg/Ca values. Yet scanning electron microscope studies of Site U1338 specimens reveal exceptional preservation of planktonic foraminifera with open pore spaces and little evidence of calcitic overgrowth on the wall surface (Fox & Wade, 2013). The interval of extensive carbonate loss at 15.6 Ma (Kochhann et al., 2016) is not part of our record, which begins at 15.5 Ma, and dissolution susceptible species are present throughout (Fox & Wade, 2013).

2. Materials and Methods

2.1. Sample Materials

Our study focuses on an 80-m section of lower-middle Miocene sediments from 350 to 430 m composite depth (mcd) from Site U1338. Pälike et al. (2012) indicate that the paleo latitude of Site U1338 is within ±2° latitude of the equator. The sediments consist of white, pale yellow, and very pale brown nannofossil ooze, grading to nannofossil and calcareous chalk (Pälike et al., 2010). For planktonic foraminiferal geochemical analyses, we use the same samples used for benthic foraminiferal stable isotope analysis in Holbourn et al. (2014), ~630 samples were analyzed at 10 cm intervals providing a ~3 kyr temporal resolution.

To assess preservation, selected specimens of planktonic foraminifera were mounted on SEM stubs, coated with gold, and inspected using a FEI Quanta 650 SEM at the University of Leeds, UK. After imaging their external surfaces at low and high resolution, several tests were broken using moderate pressure under a glass slide, and the fragments were used for the investigation of internal surfaces and test walls in cross-section (Figure 2).

2.2. Stable Isotopes

Oxygen and carbon isotope ratios ($\delta^{18}O$, $\delta^{13}C$) were measured on 10–12 shells of mixed-layer dwelling species *Globigerinoides subquadratus* from the 250 to 315 μm size fraction from 425 meters composite depth (mcd) until its extinction at 390 mcd. Analyses then continue with *Globigerinoides* spp. until 350 mcd. In a few samples, where foraminiferal density was low, only 5–7 specimens were analyzed. Analyses were made with a VG Optima mass spectrometer with multi prep device at the British Geological Survey, Keyworth, UK. When picking shells, care was taken to exclude individuals with broken or missing chambers, although preservation of specimens was generally excellent (Fox & Wade, 2013). The external reproducibility of our measurements is ±0.07‰ and ±0.05‰ for $\delta^{18}O$ and $\delta^{13}C$, respectively. To examine the reproducibility of the results, duplicate measurements were made on 35 samples (5%), which indicate mean reproducibility better than ±0.12‰ and ±0.14‰ for $\delta^{18}O$ and $\delta^{13}C$, respectively. Oxygen isotope data are reported as per mil on the VPDB scale calibrated through laboratory and international standards.

At ODP Site 1146, $\delta^{18}O$ and $\delta^{13}C$ were measured by Holbourn et al. (2010) on the mixed-layer dwelling planktonic foraminifera *Globigerinoides obliquus* or *Gs. subquadratus*, using 10–20 well-preserved tests from

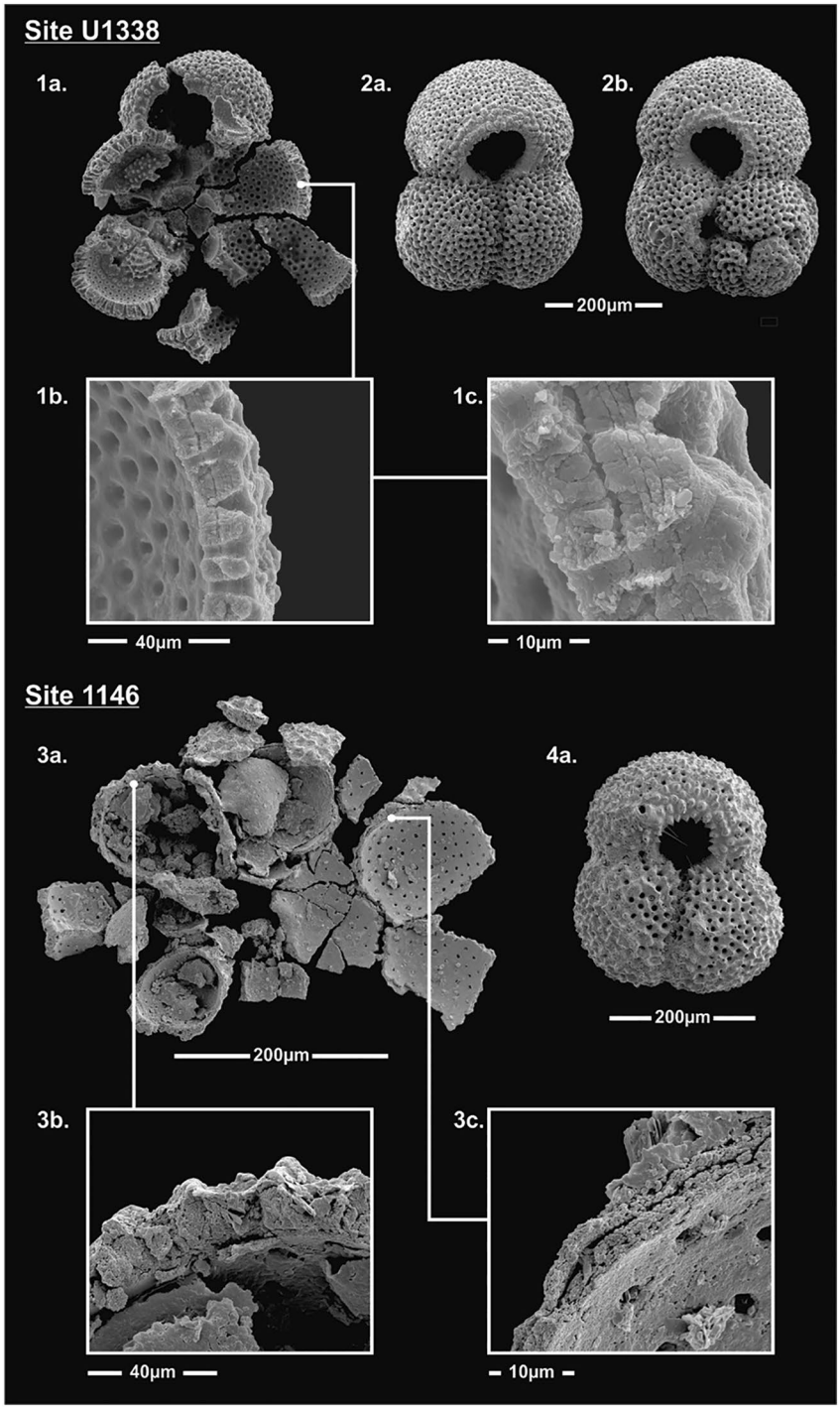

Figure 2. Scanning electron microscope images of specimens of *Globigerinoides subquadratus* from Site U1338, Sample: U1338 B-42H-2, 40–42 cm (423.04 mcd, 15.55 Ma), adapted from Fox and Wade (2013) and Site 1146, Sample: 1146-56X5, 138–142 cm (527.78 mcd, 15.19 Ma).

the size fraction 250–350 µm. Paired measurements in 51 samples indicate no significant offset in $\delta^{18}O$ and $\delta^{13}C$ between *Gs. obliquus* and *Gs. subquadratus*. Detailed methods are outlined in Holbourn et al. (2010). $\delta^{13}C$ data are not used here.

2.3. Mg/Ca

For Mg/Ca analyses, we selected 25–35 specimens of *Trilobatus quadrilobatus* (140–550 μg) from the 250 to 315 μm size fraction; the same size fraction as used for $\delta^{18}O$ analysis, to minimize size-related intraspecific elemental variation (Elderfield et al., 2002). Analyses were performed on 86 samples over the studied interval. The tests were gently crushed and subsequently cleaned according to the protocol of Martin and Lea (2002) to remove clays. Cleaning included a reductive step with hydrazine to remove Mn-(hydr)oxides. Samples were measured on an ICP-AES device at Christian-Albrechts-Universität zu Kiel, Germany. Analytical precision is ~1.1%, based on measurements of an internal laboratory standard. Replicate Mg/Ca measurements revealed an average standard deviation of ~0.08 mmol/mol. Adequate cleaning is indicated by very low Fe/Ca, Al/Ca and Mn/Ca ratios.

For ODP Site 1146 up to 40 tests of *Gs. subquadratus* or *Gs. obliquus* from the 250 to 350 μm size fraction were analyzed by Holbourn et al. (2010). Specimens were gently crushed and cleaned following methods outlined by Martin and Lea (2002), which include a reductive step with hydrazine to remove Mn-(hydr) oxides. Details of the procedure are outlined in Holbourn et al. (2010).

2.4. Planktonic Foraminiferal Taxonomy and Ecology

Trilobatus quadrilobatus is a multi-chambered and photosymbiont bearing species, which forms part of the *T. sacculifer* plexus (Poole & Wade, 2019). This species first appeared in the early Miocene (Subzone M1a), and *T. quadrilobatus*, *sacculifer*, and *trilobus* morphotypes are all found in the modern ocean produced by the same species (Andre et al., 2013). Many studies point to a depth habitat within the upper ~80 m of the water column for *T. sacculifer* (Fairbanks et al., 1982; Steph et al., 2009), which make this an ideal species to reconstruct SSTs in the equatorial Pacific Ocean.

Globigerinoides subquadratus is often considered to be a homeomorph of *Gs. ruber* (Chaisson & Leckie, 1993; Pearson, 1995), which is a common and ubiquitous species in tropical/subtropical biogeographic provinces (Bé & Torderlund, 1971). *Globigerinoides subquadratus* first appeared within the M1a subzone (22.44–22.96 Ma, base of Aquitanian stage) and becomes extinct near the base of Zone M11 (~11.5 Ma, in the Tortonian stage) (Spezzaferri et al., 2018; Wade et al., 2011). Isotopic data indicate a similar depth habitat for *Gs. subquadratus* and *Gs. ruber* (Pearson, 1995), which is one of the shallowest dwelling species (<50 m) of all planktonic foraminifera (Fairbanks et al., 1982; Ravelo & Fairbanks, 1992). Both *G. ruber* and *G. subquadratus* are extensively used to reconstruct past SST and salinity variations.

Globigerinoides obliquus is a long-ranging, tropical to subtropical species, which first appeared in the early Miocene (Kennett and Srinivasan, 1983). Duplicate measurements of *Gs. obliquus* and *Gs. subquadratus* at Site 1146 indicate no offsets in $\delta^{18}O$ and $\delta^{13}C$ between these two species (Holbourn et al., 2010). This suggests that these two species had a similar depth habitat within the mixed layer.

2.5. Mg/Ca Paleotemperature Calculation

To investigate the influence of temperature on the upper ocean oxygen isotope gradient between the eastern and western Pacific Oceans, Mg/Ca analyses were performed on selected samples at Site U1338 to compare with the Site 1146 records (Holbourn et al., 2010). The planktonic species *T. quadrilobatus* forms part of the *sacculifer* plexus (Poole & Wade, 2019; Spezzaferri et al., 2018). Therefore, the conversion of *T. quadrilobatus* Mg/Ca ratios to SSTs was carried out using the *T. sacculifer* calibration (Anand et al., 2003):

$$\frac{Mg}{Ca} = 0.347\left(\pm 0.011\right)e^{0.09\left(\pm 0.003\right)T} \quad (1)$$

The lengthy residence times of Ca (~1.1 Myr) and Mg (~13 Myr) (Broecker et al., 1982) suggests that Mg/Ca of seawater (Mg/Ca_{sw}) is unlikely to have varied significantly over the duration of our 2.3 Myr record. However, Mg/Ca_{sw} may have been considerably different in the Miocene compared to the present day values of 5.2 mmol/mol (Evans Mueller, 2012). Attempts have been made to reconstruct Mg/Ca_{sw} over time using geochemical models (Fantle & DePaolo, 2005, 2006; Stanley & Hardie, 1999), echinoderm skeletons

(Dickson, 2002, 2004), low-resolution analyses of fluid inclusions in marine evaporites (Horita et al., 2002; Lowenstein et al., 2001; Sime et al., 2007) and carbonate veins precipitated in oceanic basalt (Coggon et al., 2010). Whilst these various reconstructions agree that Mg/Ca_{sw} was lower during the Miocene than today, its precise value remains uncertain and the long-term evolution of Mg/Ca_{sw} is still unclear. For this study the fluid inclusion value of 3.43 mmol/mol is used in the paleotemperature equation (at both sites) for consistency with the recent Miocene study by Sosdian et al. (2020); following the calculations outlined in their methods, we used the *T. sacculifer* calibration of Anand et al. (2003) ($A = 0.09$, $B = 0.347$) for *T. quadrilobatus* and applied a power constant of 0.41 for *T. sacculifer* based upon the available data for this species (Delaney et al., 1985; Evans & Mueller, 2012). *T. quadrilobatus* SST estimates were therefore calculated from the following equation (Sosdian et al., 2020):

$$\frac{Mg}{Ca_{\text{foram}}} = 0.293\, e^{0.09T} \tag{2}$$

In addition to changes in seawater Mg/Ca, it has been suggested that a pH correction is necessary for estimating SST (Evans et al., 2016; Gray & Evans, 2019). However, as Mg/Ca ratios in the *T. sacculifer* plexus are unaffected by changes in ocean pH (Allen et al., 2016; Drury et al., 2018), no correction was applied in this study.

2.6. Site Location Water Depth

The direct comparison of two records from sites with contrasting paleo-water depths (~2,000 m at Site 1146 and 3,000–3,500 m at Site U1338; Holbourn et al., 2010; Pälike et al., 2012) and thus saturation state, is a potential source of uncertainty in Mg/Ca paleotemperature calculations. In Figures 3 and 5 SST estimates are presented that correct for the potential effects of dissolution on Mg/Ca ratios due to decreasing $[CO_3^{2-}]$ with increasing water depth (Dekens et al., 2002; Elderfield et al., 2006; Rosenthal et al., 2006). This is achieved by using the Pacific Ocean depth calibration of Dekens et al. (2002) for *T. sacculifer* for Site U1338 and the Pacific Ocean depth calibration for *Gs. ruber* for Site 1146.

Trilobatus quadrilobatus SST estimates corrected for potential effects of paleo-water depth can be calculated from the following equation:

$$\frac{Mg}{Ca} = 0.293\, e^{0.09\left[T - 0.36\left(\text{core depth km}\right)\right]} \tag{3}$$

Globigerinoides subquadratus/Gs. obliquus SST estimates corrected for potential effects of paleo-water depth can be calculated from the following equation:

$$\frac{Mg}{Ca} = 0.293\, e^{0.09\left[T - 0.61\left(\text{core depth km}\right)\right]} \tag{4}$$

At Site U1338, the uncertainty in estimating changes in sea surface temperatures during the MMCT with planktonic foraminiferal Mg/Ca is about ±~1°C (σ1), largely due to the variability among replicated samples (estimated here to be ~0.9°C) and the error associated with the temperature sensitivity of the calibration (1.13°C; Anand et al., 2003). We estimate the combined error for absolute SSTs for Site U1338 to be ±2°C.

Holbourn et al. (2010) report the uncertainty of paleotemperature estimates at Site 1146 to be ±1.2°C. This combines the standard deviation deduced from the calibration study (±1.13°C; Anand et al., 2003) and the analytical error of the Mg/Ca measurement. No correction was applied for the reductive step applied in our cleaning protocol, which generally results in a small decrease in Mg/Ca, leading to temperature underestimation of up to ~0.6°C (Rosenthal et al., 2004). Changes in salinity may also have altered Mg/Ca reconstructed temperatures, however, Tierney et al. (2019) suggest that sensitivity is low between 33 and 38 PSU, we therefore did not make any adjustments for salinity changes.

2.7. Site 1146 Sensitivity of Reconstructed SSTs

We applied several equations to examine the sensitivity of reconstructed SSTs at Site 1146 (Figure 3). Holbourn et al. (2010) used the Anand et al. (2003) equation to calculate SSTs at Site 1146, this gives rise to SSTs

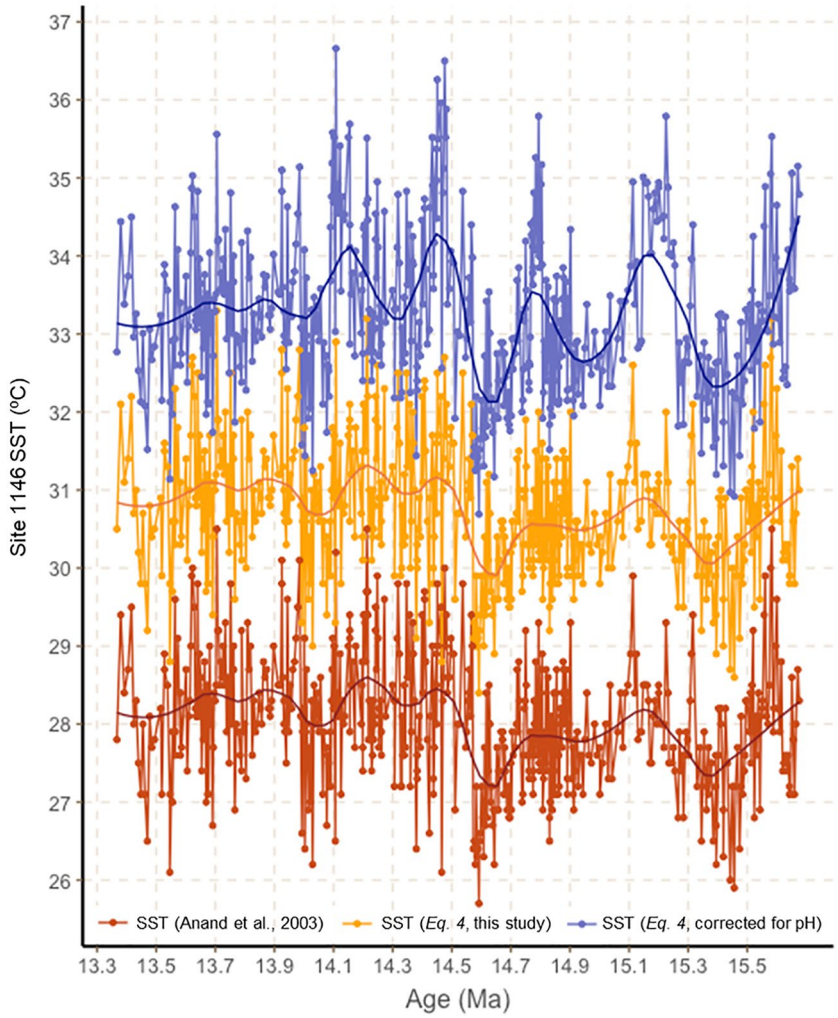

Figure 3. SST estimates for Site 1146 derived from Mg/Ca analysis. SST estimates are based on a range of different calibrations (see Materials and Methods). Red line illustrates temperature estimates following methods in Anand et al. (2003) as presented in Holbourn et al. (2010), The orange line represents SST estimates from Equation 4 presented in this study, which accounts for water depths and species specific calibrations. The blue line illustrates SST estimates following Equation 3 with additional correction for pH.

averaging 28°C, varying by 5°C between 30.5°C and 25.5°C (Figure 3). Adjusting for dissolution, following the equation of Dekens et al. (2002), average SSTs increase by 3°C, with a mean of 31°C, fluctuating between 33°C and 28°C. By adjusting for pH (Figure 3), the variability in SSTs becomes more extreme, between 36.5°C and 31°C with mean SSTs of 33°C. Equation 4 without the pH correction, is more consistent with the current understanding of mid Miocene temperatures and seasonal variation in the subtropics (Herold et al., 2012).

2.8. Surface Seawater $\delta^{18}O$

To determine changes in surface seawater $\delta^{18}O$ ($\delta^{18}O_{sw}$) and the impact of evaporation and precipitation changes, we used our paired planktonic foraminifera Mg/Ca temperatures and $\delta^{18}O$ to reconstruct $\delta^{18}O_{sw}$ at Site U1338. We corrected $\delta^{18}O_{sw}$ for ice volume by applying an ice volume value of 0.58‰ from the base of the record to 13.9 Ma, and 1.18‰ from 13.7 Ma and younger following Modestou et al. (2020). For the 200 kyr between 13.9 to 13.7 Ma we applied a linear correction of 0.003‰ per 1 kyr.

3. Results

At the east Pacific Site U1338, planktonic foraminiferal $\delta^{18}O$ fluctuates between ~−1.8‰ and −0.4‰ (Figure 4b). The $\delta^{18}O$ record of Site 1146 shows higher amplitude variability than Site U1338 with $\delta^{18}O$ values fluctuating between ~−3.6‰ and −2.0‰. Comparison of the planktonic foraminiferal $\delta^{18}O$ records between Site U1338 and Site 1146 reveals an average offset of ~1.5‰, with the east Pacific recording the more positive values (Figures 4a–4b). Across Mi-3, while there is a 1‰ increase in benthic foraminifera $\delta^{18}O$, we do not see accompanying changes in the planktonic foraminifera $\delta^{18}O$ of corresponding magnitude. Given that ice volume changes would impact $\delta^{18}O$ in both planktonic and benthic foraminifera at the same time and to the same extent, the minor $\delta^{18}O$ variations of in the planktonic foraminifera data would suggest the $\delta^{18}O$ record is counterbalanced by surface water salinity variations.

Separation of the various components of the $\delta^{18}O$ signal (temperature, salinity, ice volume) are required to improve understanding of the processes and feedbacks at work during this interval of climatic transition. The measured Mg/Ca ratios for the mixed layer dwelling species *T. quadrilobatus* at Site U1338 range from approximately 2.5 to 3.8 mmol/mol, giving a mean value of ~3.2 mmol/mol and are consistently ~1 mmol/mol lower than those at Site 1146 (Figure 5e).

Mg/Ca-derived SSTs following corrections (with adjusted paleo water depth) average at 26.4°C ± 2°C for Site U1338 (Figure 5d), these values are 2.8°C warmer than SSTs calculated following Equation 2. Similarly, Mg/Ca-derived SSTs calculated for Site 1146 following corrections are 2.6°C warmer than those originally presented in Holbourn et al. (2010). At Site 1146, SSTs calculated using Equation 4 vary between ~28.3°C and 33.2°C with a mean temperature of 30.6°C, whereas at Site U1338 the SST record ranges from 23.6°C to 28.9°C with an average temperature of 26.4°C (Figure 5d). The temperature offset between Site 1146 and Site U1338 remains present in both the paleo water depth corrected and the uncorrected SST records.

Our corrected Mg/Ca SSTs in conjunction with planktonic foraminifera $\delta^{18}O$, allows for the calculation of $\delta^{18}O_{sw}$. At Site U1338, $\delta^{18}O_{sw}$ averages 0.75 ± 0.25‰ from 15.5 to 13.7 Ma (Figure 5a), and decreases to 0.0‰ at 13.45 Ma. At Site 1146, $\delta^{18}O_{sw}$ is consistently lighter than at Site U1338 with mean values of 0.00 ± 0.31‰ from 15.5 to 13.9 Ma, values become more positive and reach 0.75‰ at 13.8 Ma, before decreasing to −0.55‰ at 13.45 Ma. The $\delta^{18}O_{sw}$ gradient between the two sites is approximately 0.75‰ from 15.5 to 14.2 Ma, decreasing to 0.25‰ in the younger part of our record.

4. Discussion

4.1. Foraminiferal Preservation and Calcification Depth

Dissolution has been shown to impact foraminiferal Mg/Ca values (Dekens et al., 2002; Fehrenbacher et al., 2006; Regenberg et al., 2006); indeed, a recent study on bottom water temperatures by Kochhann et al. (2016) found evidence for minor carbonate dissolution at the event of peak warmth (15.6 Ma) at Site U1338. However, high resolution SEM analysis of planktonic foraminiferal specimens from Site U1338 reveals exceptional preservation of the original test wall texture and no visible etching of the wall surfaces (Figure 2) at 15.56 Ma, where the Site U1338 planktonic foraminiferal record begins. A detailed study of Site U1338 planktonic foraminiferal assemblages also reveals numerous dissolution susceptible species are present throughout the studied interval (Fox & Wade, 2013). Furthermore, a reconstruction of the paleo-water depth and the carbonate compensation depth (CCD) in the equatorial Pacific suggests that Site U1338 has been above the CCD from 20 Ma to the present day (Pälike et al., 2012). Preservation at Site 1146 is recorded as “good” to “very good” over the studied interval, this means <20% fragmentation of foraminifera specimens and no visible evidence of etching. Whilst detailed SEM analyses conducted on multiple specimens reveal minimal recrystallization on foraminifer tests at both Sites U1338 and 1146 (Figure 2), the SST data presented in Figure 5 have been calculated using a dissolution correction (Equation 3) to ensure the potential effects of contrasting water depths on our specimens has been considered. However, we argue that the impact was minimal at Site U1338, and that preservation of foraminiferal specimens at Site U1338 is comparable and often superior to those found at the shallower Site 1146 (as illustrated in Figure 2).

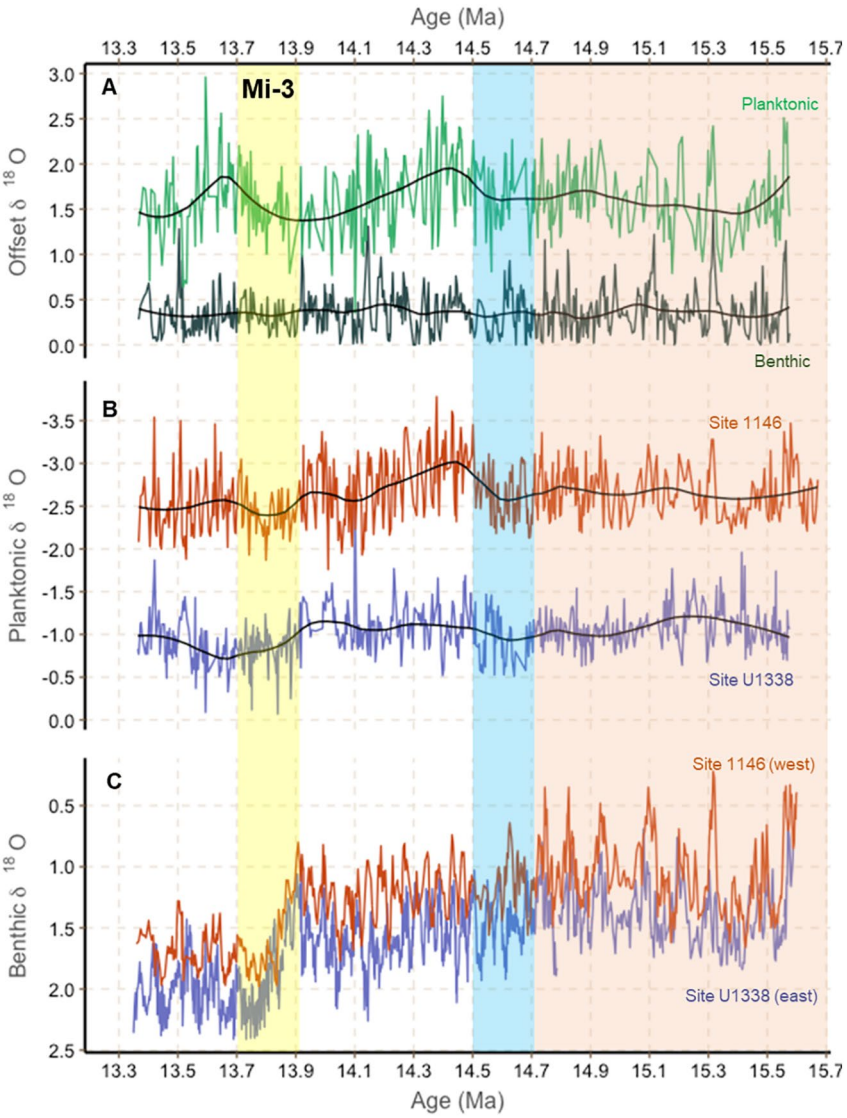

Figure 4. Stable isotope data for the tropical Pacific for 13.3–15.6 Ma. (a) Calculated $\delta^{18}O$ offset between Site U1338 and 1146, light green line represents planktonic foraminiferal data, dark green line represents benthic foraminiferal data. The black line represents a local weighted regression line (b) Planktonic foraminiferal $\delta^{18}O$ from Site U1338 (blue line, this study) and Site 1146 (red line, Holbourn et al., 2010). (c). (c) Benthic foraminiferal $\delta^{18}O$ from Site U1338 (Holbourn et al., 2014) and Site 1146 (Holbourn et al., 2010). Yellow band marks Mi-3 event ~13.9–13.8 Ma. Blue band marks global cooling step at ~14.6–14.7 Ma. Darker orange band marks Miocene Climate Optimum.

Mg/Ca estimates for Site U1338 are in good agreement, though slightly lower (~1°C) than SST reconstructions for the same site using alkenones, which record temperatures of ~28°C during this interval (Rousselle et al., 2013) (Figure 5d). Whilst these data are well within the uncertainty of each other, the calcification depth of *T. quadrilobatus* may also have played a role in the difference in SST estimates calculated from alkenones (Rousselle et al., 2013) and foraminiferal Mg/Ca (this study) at Site U1338.

4.2. Impact of Ice Sheet Expansion at 13.9–13.8 Ma

Comparison of the benthic foraminiferal $\delta^{18}O$ records from Sites U1338 and 1146 (Figure 4c) reveals a strong coherence between the two benthic foraminiferal $\delta^{18}O$ datasets, in terms of amplitude and timing of both the long-term trends and short-term cycles. During the middle Miocene (~16–11.6 Ma) the global climate shifted from an interval of global warmth, the "Miocene Climatic Optimum" (MCO), to a period

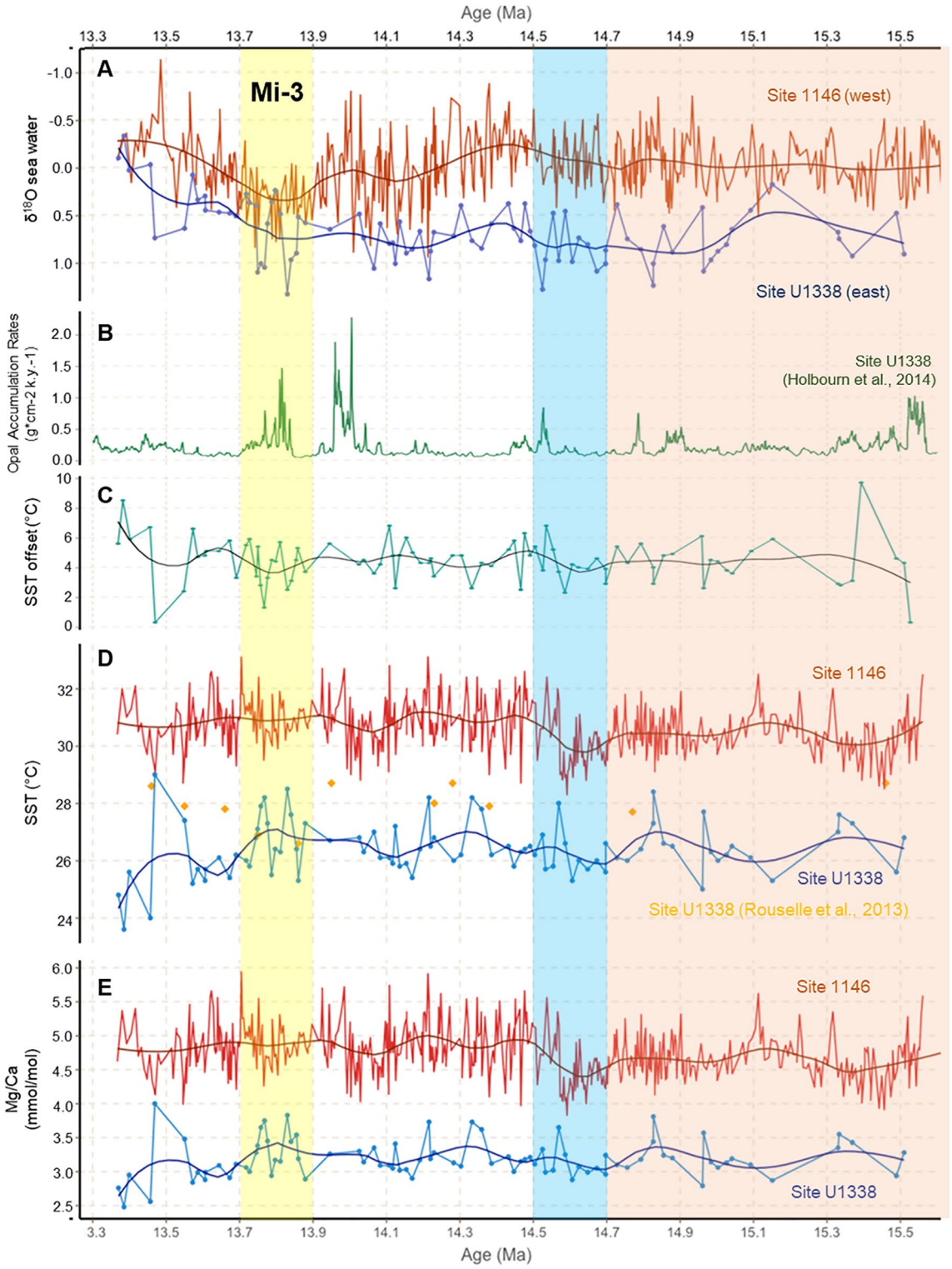
Age (Ma)
13.3
13.5
13.7
13.9
14.1
14.3
14.5
14.7
14.9
15.1
15.3
15.5
A
Mi-3
Site 1146 (west)
Site U1338 (east)
δ18O sea water
-1.0
-0.5
0.0
0.5
1.0
B
Site U1338
(Holbourn et al., 2014)
Opal Accumulation Rates
(g*cm-2 k.y.-1)
2.0
1.5
1.0
0.5
0.0
C
SST offset (°C)
10
8
6
4
2
0
D
Site 1146
Site U1338
Site U1338 (Rouselle et al., 2013)
SST (°C)
32
30
28
26
24
E
Site 1146
Site U1338
Mg/Ca
(mmol/mol)
6.0
5.5
5.0
4.5
4.0
3.5
3.0
2.5
3.3
13.5
13.7
13.9
14.1
14.3
14.5
14.7
14.9
15.1
15.3
15.5
Age (Ma)

Figure 5.

of stepwise cooling during the MMCT. A major expansion of the EAIS occurred at ~13.9–13.8 Ma following an initial cooling step at ~14.7–14.6 Ma (e.g., Holbourn et al., 2007; Shevenell et al., 2004; Westerhold et al., 2005). The major glaciation at ~13.9–13.8 Ma or Mi-3 event, highlighted on Figure 4, is recorded as a ~1‰ increase in the benthic foraminiferal $\delta^{18}O$ at both sites.

At Site U1338 Mg/Ca derived SSTs average 27°C between 15.5 and 13.7 Ma. Surprisingly, we do not see any decrease in SSTs in the eastern or western Pacific associated with Mi-3 (Figure 5d). Minimal sea surface cooling occurs between 13.9 and 13.6 Ma, whereas the enrichment in benthic foraminiferal $\delta^{18}O$ marks the onset of a long-term climate shift at high latitudes, primarily due to deep ocean temperature cooling and polar ice growth. The lack of SST excursion at Mi-3 at low latitude sites, as recorded in both Mg/Ca and alkenone-based temperature proxies across the interval of ice sheet expansion (Figure 5d), contrasts with high latitude records from the Southern Ocean, which indicate a ~6°C–7°C cooling (Shevenell et al., 2004), thus signifying a large increase in the meridional temperature gradient, as the Earth transitioned toward icehouse conditions. Furthermore, the divergence between the degree of positive $\delta^{18}O$ change at ~13.9–13.8 Ma in the surface and deep water records suggests that variations in local salinity are also imprinted on the surface $\delta^{18}O$ data, as indicated by the $\delta^{18}O_{sw}$ records (Figure 4a).

Following Mi-3, SSTs in the eastern Pacific (Site U1338) decreased to ~26°C at 13.5 Ma and to ~25°C in the youngest part of our record (13.35 Ma), although there is some variability with two of the warmest SST values (28°C) occurring at 13.5 Ma. The SST offset of ~4°C between Sites 1146 and U1338 remained stable for over 1 million years (Figure 5c), however, the overall reduction in SSTs at Site U1338 after 13.7 Ma results in an increase in SST gradient to 7°C in the youngest part of our record. Significantly, the decrease in Mg/Ca SSTs occurs after Mi-3, and not in tandem with the benthic foraminiferal $\delta^{18}O$ changes. The sea surface cooling recorded by planktonic foraminifera Mg/Ca is not synchronous with ice growth and deep sea cooling inferred from the benthic foraminiferal $\delta^{18}O$ record, but occurs ~150 kyr later (Figure 4c). The delayed SST cooling at Site U1338 is inconsistent with low-latitude records from ODP Sites 806 and 761, where surface cooling occurs synchronously with deep water temperature decrease and ice growth (Sosdian & Lear, 2020). The delayed SST cooling at Site U1338, indicates a heterogeneous temperature response across Mi-3 and suggests that changes in ocean circulation played a role.

The delayed 2°C cooling between ~13.7 and 13.4 Ma displayed in the Mg/Ca derived SST record at Site U1338 (Figure 5d) indicates that deep sea cooling and Antarctic ice growth preceded the SST decrease. This contrasts with the dynamics of the Eocene-Oligocene Transition (34–33.5 Ma), when SSTs decreased prior to the interval of major ice sheet expansion (Lear et al., 2008; Wade et al., 2012). Unlike the EOT, Mi-3 is not associated with a turnover in plankton assemblages.

4.3. Evolution of Pacific Ocean Temperature and $\delta^{18}O$ Gradients

The planktonic foraminiferal $\delta^{18}O$ gradient between Sites U1338 and 1146 averages ~1.5‰, with more positive values in the east Pacific (Site U1338). Using our Mg/Ca results, ~1‰ of the offset in planktonic foraminiferal $\delta^{18}O$ between the two sites can be explained by temperature (assuming 0.22‰ per °C, Kim & O'Neil, 1997). The remaining 0.5‰ must therefore relate to differences in regional evaporation-precipitation budgets and/or ocean circulation. On the basis of the modern $\delta^{18}O$-salinity relationship (Conroy et al., 2014), a change of 0.5‰ in the $\delta^{18}O$ of seawater reflects a surface salinity shift of between 1 and 1.5 p.s.u (Stott et al., 2004). Present-day surface water salinities (Figure 1) are lower in the western tropical Pacific Ocean (~33.5 p.s.u at Site 1146) and increase toward the eastern part of the basin (~35 p.s.u at Site U1338).

Figure 5. (a) $\delta^{18}O_{sw}$ calculated from Site U1338 (blue line, this study) and Site 1146 (red line), the dark red and dark blue lines represent a local weighted regression line (b) Opal accumulation rate for Site U1338 (Holbourn et al., 2014). (c) Calculated temperature offset between Sites U1338 and 1146. Dashed line represents present day temperature offset between Sites 1146 and U1338. (d) SST reconstructions from Mg/Ca ratios measured on planktonic foraminifera following Equation 3. Site 1146 data (red line) from Holbourn et al. (2010), Site U1338 data (blue line), this study. Orange points represent SST estimates for Site U1338 from alkenones (Rousselle et al, 2013). The calibration error for reconstructed temperatures is ~2°C for Mg/Ca. (e) Mg/Ca ratio of planktonic foraminifera. Yellow band marks Mi-3 event ~13.9–13.8 Ma. Blue band marks global cooling step at ~14.6–14.7 Ma. Darker orange band marks Miocene Climate Optimum. The black line represents a local weighted regression line.

Transient increases in the planktonic foraminiferal $\delta^{18}O$ gradient between Sites 1146 and U1338 following the global cooling steps at ~14.7–14.6 Ma and ~13.9–13.8 Ma (Figure 3b) additionally support latitudinal shifts or intensification of the Intertropical Convergence Zone (ITCZ) coupled to waxing and waning of the WPWP through time. The divergence between the benthic and planktonic foraminiferal $\delta^{18}O$ gradients after ~14.6 and ~13.8 Ma (Figure 4b) is primarily driven by decreases in planktonic foraminiferal mean $\delta^{18}O$ values at Site 1146. These decreases, also clearly expressed in the $\delta^{18}O$ seawater record at Site 1146, have been related to rises in regional precipitation, associated with intensification of the Southeast Asian monsoonal subsystem following global cooling (Holbourn et al., 2010). These temporal changes in local precipitation and $\delta^{18}O$ seawater patterns also imply that the Southeast Asian monsoonal climate was highly sensitive to changes in the interhemispheric thermal gradient during the middle Miocene.

The average temperature offset between the records from Sites U1338 and 1146 (Figure 5) is approximately ~4°C, comparable with the modern temperature difference between these two sites (Figure 1). However, the spatial extent of the WPWP may have differed on a warmer Miocene Earth, with a substantially reduced latitudinal thermal gradient (e.g., Fedorov et al., 2015). Middle Miocene temperatures at Site 1146 were ~2°C–3°C warmer than present-day, supporting a northwards expansion of the WPWP throughout this extended interval of warmth. During the MMCT, differing rates of cooling between hemispheres following Antarctic glacial expansion probably favored a northwards displacement of the annual mean position of the ITCZ, away from the cooler hemisphere (e.g., Chiang & Bitz, 2005; Broccoli et al., 2006; Yang et al., 2020). This northwards shift would have maintained relatively warm temperatures at Site 1146 during the MMCT. In the eastern equatorial Pacific Ocean, temperatures were also ~2°C–3°C warmer than present through the MCO and MMCT, suggesting that upwelled intermediate waters had different properties and origin compared to today.

4.4. Eastern Equatorial Pacific Paleoceanography

The paleoceanography of the eastern equatorial Pacific Ocean is complex, and sea surface conditions prior to 8 Ma are not well known or understood, due to a lack of high resolution proxy records (Drury et al., 2018). Frontal systems, upwelling and the cold tongue are all responsive to changes in atmospheric circulation, particularly the trade winds, which alter with changes in the meridional gradients (for instance high latitude cooling associated with Mi-3). Furthermore, the volume of throughflow through the Central American Seaway, which would impact salinity gradients in the EEP, is not well constrained. From 15.5 to 13.3 Ma, Site U1338 was located ~1° south of the equator (Pälike et al., 2010), a region affected by the seasonal migration of the ITCZ. The EEP is a region of low sea surface salinity (~33.5–34‰) due to high annual rainfall, low evaporation and advection of low salinity water (Alory et al., 2012; Martins & Stammer, 2015). Salinity changes both temporally and spatially (Melnichenko et al., 2019), and low salinity anomalies in the EEP are driven by strong and transient storms (Riser et al., 2019). Salinity interactions between advecting water and heavy rainfall are varied, and subject to entrainment and nonlinear effects (Martins & Stammer, 2015).

The “cold tongue” (Wyrtki, 1981) is an area of cool SSTs within the EEP. It is caused by divergence of surface Ekman currents resulting in water upwelling from the subsurface and advecting from the east (Zheng et al., 2012). The strength of the cold tongue has been shown to vary on glacial-interglacial timescales (Koutavas & Lynch-Stieglitz, 2004). Shoaling of the EEP thermocline and expansion of the cold tongue have been linked to cooling and the expansion of subpolar oceans on more recent timescales (Martinez-Garcia et al., 2010), though processes that influence the range and intensity of the cold tongue are not well understood. Whilst a cold tongue comparable to the modern may not have developed until the late Miocene or younger (Liu et al., 2019; Steph et al., 2010), there is widespread evidence that upwelling in the EEP initiated in the mid Eocene (Lyle et al., 2002; Moore et al., 2004; Wade et al., 2020; Zhang et al., 2017), thus, the EEP would have developed a proto-cold tongue, due to advection of cold, deep water.

The cooling and freshening of the EEP, could have been driven by enhanced advection of deep waters in response to high latitude cooling and strengthening of the trade winds. Intensification of upwelling is suggested at 14 and 13.8 Ma by Holbourn et al. (2014) based on the productivity proxies of opal mass accumulation rates from X-ray fluorescence (XRF) scanning, silica content and carbon isotopes. However, our SST cooling is not associated with higher biogenic opal accumulation rates (Figure 5b), thus the data do

not support enhanced upwelling at 13.75 Ma and younger as the mechanism for the ~2°C SST cooling. The decrease in Mg/Ca values and $\delta^{18}O_{sw}$ is not synchronous with the major benthic foraminifera $\delta^{18}O$ increase (Mi-3) (Figure 4), or with high latitude SST changes (Shevenell et al., 2008), suggesting that the EEP surface water cooling and freshening are in response to the initiation of the new climate regime of the icehouse mode. We suggest that alterations in wind patterns changed the boundaries between frontal systems and caused SST cooling in the EEP.

4.5. Changes in the Hydrological Cycle During the Middle Miocene

We find a freshening of EEP surface waters after Mi-3, suggesting a change in the precipitation-evaporation balance. It is surprising that the cooling and change in $\delta^{18}O_{sw}$ occurred after 13.7 Ma, postdating the deep water temperature and Antarctic ice volume changes. A freshening of ocean surface waters has now been recorded at multiple sites associated with/around Mi-3. These include western Pacific Sites 1146 (Holbourn et al., 2010) and 806 (Sosdian & Lear, 2020), eastern Pacific Site U1338 (this study) and Indian Ocean Site 761 (Sosdian & Lear, 2020). These global changes in low-latitude surface water $\delta^{18}O_{sw}$ suggest that major disruptions of the hydrological cycle and global precipitation patterns accompanied ice sheet expansion in the mid Miocene.

The meridional gradient and heat transfer between the hemispheres have a direct influence on the position of the ITCZ (McGee et al., 2014). The drop in $\delta^{18}O_{sw}$ of this magnitude (0.75‰) in the EEP surface waters (13.8–13.35 Ma), is unlikely to have been driven solely by increased precipitation, and hydrological changes would not explain the reduction in SSTs. High latitude ice cover has been shown to impact EEP through wind-evaporation-SST feedbacks (Chiang & Bitz, 2005). Southern hemisphere cooling and Antarctic ice expansion at ~13.9–13.8 Ma was associated with a general improvement in deep water ventilation and strengthening of the meridional overturning circulation (Holbourn et al., 2013). These changes likely caused a re-organization of atmospheric circulation that led to major changes in the intensity and distribution of regional precipitation, ITCZ migration, and expansion of the cold tongue following Mi-3. The surface water cooling and freshening is more probably due to changes in surface ocean currents and frontal systems in response to changes in the meridional gradient. We suggest that increased meridional gradients and enhanced atmospheric transport led to dynamic reorganization in the hydrological cycle, with increased precipitation in the tropics, coupled with alterations in surface currents in the EEP. Further research is currently underway to extend the planktonic foraminifera isotope and Mg/Ca record at Site U1338 to determine the asymmetry of the western to eastern Pacific changes through the middle and late Miocene, and whether the reduction in $\delta^{18}O_{sw}$ represents a short or longer term modification in the EEP.

5. Conclusions

Here, we present a new middle Miocene record of planktonic foraminiferal $\delta^{18}O$ and Mg/Ca for the eastern equatorial Pacific Ocean (IODP Site U1338). The Mg/Ca derived SST records generated for Sites U1338 and 1146 (Figure 5) reveal a clear temperature asymmetry of ~4°C across the Pacific Ocean throughout the middle Miocene (15.6–13.3 Ma). This implies that the oceanographic features, such as a relatively shallow thermocline and upwelling, were present and active in the eastern Pacific Ocean during the MCO, the warmest interval of the Neogene. Furthermore, the E-W gradient was unaffected by major Southern Hemisphere ice growth and the transition to a substantially colder climate mode after ~13.9 Ma. Hydrological changes and variations in frontal systems caused a freshening of the sea surface following Mi-3. Significantly, sea surface cooling in the equatorial Pacific is not synchronous with the major benthic foraminifera d18O shifts, but is delayed by ~150 kyr. Throughout our records (15.6–13.3 Ma), the E-W gradient never approaches zero, as implied for a “permanent El Niño” like state.

Data Availability Statement

The data that support the findings of this study are openly available via the National Geoscience Data Center (NDCD), Data ID: 164526. https://webapps.bgs.ac.uk/services/ngdc/accessions/index.html#item164526.

Acknowledgments
This research was supported by UK Natural Environment Research Council (NERC) reference number NE/I528750/1 and a UK-IODP Rapid Response Award to Lyndsey Fox, NERC grant NE/G014817 and NERC Isotope Geosciences Facilities (IP-1345-1112 and IP-1239-0511) to Bridget Wade, and the Deutsche Forschungsgemeinschaft Grant HO233/1 to Ann Holbourn. Samples were provided by the Integrated Ocean Drilling Program (IODP). IODP is sponsored by the U.S. National Science Foundation and participating countries. We thank Paul Minton, Anna Joy Drury, Mark Leckie and David Evans for discussion, and Marcus Regenberg for his assistance with Mg/Ca analyses. We are grateful to Yige Zhang and Flavia Boscolo-Galazzo for helpful constructive reviews that greatly improved the manuscript.

References

Allen, K. A., Hönisch, B., Eggins, S. M., Haynes, L. L., Rosenthal, Y., & Yu, J. (2016). Trace element proxies for surface ocean conditions: A synthesis of culture calibrations with planktic foraminifera. *Geochimica et Cosmochimica Acta*, *193*, 197–221. https://doi.org/10.1016/j.gca.2016.08.015

Alory, G., Maes, C., Delcroix, T., Reul, N., & Illig, S. (2012). Seasonal dynamics of sea surface salinity off Panama: The far eastern Pacific fresh pool. *Journal of Geophysical Research*, *117*, C04028. https://doi.org/10.1029/2011JC007802

Anand, P., Elderfield, H., & Conte, M. H. (2003). Calibration of Mg/Ca thermometry in planktonic foraminifera from a sediment trap time series. *Paleoceanography*, *18*(2), 1050. https://doi.org/10.1029/2002pa000846

André, A., Weiner, A., Quillévéré, F., Aurahs, R., Morard, R., Douady, C. J., et al. (2013). The cryptic and the apparent reversed: Lack of genetic differentiation within the morphologically diverse plexus of the planktonic foraminifer Globigerinoides sacculifer. *Paleobiology*, *39*(1), 21–39. https://doi.org/10.1666/0094-8373-39.1.21

Badger, M. P., Lear, C. H., Pancost, R. D., Foster, G. L., Bailey, T. R., Leng, M. J., & Abels, H. A. (2013). CO_2 drawdown following the middle Miocene expansion of the Antarctic Ice Sheet. *Paleoceanography*, *28*(1), 42–53. https://doi.org/10.1002/palo.20015

Barron, J. A., & Keller, G. (1982). Widespread Miocene deep-sea hiatuses: Coincidence with periods of global cooling. *Geology*, *10*(11), 577–581. https://doi.org/10.1130/0091-7613(1982)10<577:wmdhcw>2.0.co;2

Bé, A. W. H., & Tolderlund, D. S. (1971). Distribution and ecology of living planktonic foraminifera in surface waters of the Atlantic and Indian Oceans. In B. H. Funnell, & W. R. Riedel (Eds.), *The Micropalaeontology of the Oceans* (pp. 105–149). London: Cambridge University Press.

Broccoli, A. J., Dahl, K. A., & Stouffer, R. J. (2006). Response of the ITCZ to Northern Hemisphere cooling. *Geophysical Research Letters*, *33*, L01702. https://doi.org/10.1029/2005GL024546

Broecker, W. S., Peng, T. H., & Beng, Z. (1982). Tracers in the sea. In *Lamont-Doherty geological observatory*. Columbia University.

Chaisson, W. P., & Leckie, R. M. (1993). High-resolution Neogene planktonic foraminifer biostratigraphy of Site 806, Ontong Java Plateau (western equatorial Pacific). In *Proceedings ODP, Science Results* (Vol. 130, pp. 137–178).

Chiang, J. C. H., & Bitz, C. M. (2005). Influence of high latitude ice cover on the marine intertropical convergence zone. *Climate Dynamics*, *25*, 477–496. https://doi.org/10.1007/s00382-005-0040-5

Coggon, R. M., Teagle, D. A., Smith-Duque, C. E., Alt, J. C., & Cooper, M. J. (2010). Reconstructing past seawater Mg/Ca and Sr/Ca from mid-ocean ridge flank calcium carbonate veins. *Science*, *327*(5969), 1114–1117. https://doi.org/10.1126/science.1182252

Conroy, J. L., Cobb, K. M., Lynch-Stieglitz, J., & Polissar, P. J. (2014). Constraints on the salinity–oxygen isotope relationship in the central tropical Pacific Ocean. *Marine Chemistry*, *161*, 26–33. https://doi.org/10.1016/j.marchem.2014.02.001

DeDeckker, P. (2016). The Indo-Pacific warm pool: Critical to world oceanography and world climate. *Geoscience Letters*, *3*(1), 1–12. https://doi.org/10.1186/s40562-016-0054-3

Dekens, P. S., Lea, D. W., Pak, D. K., & Spero, H. J. (2002). Core top calibration of Mg/Ca in tropical foraminifera: Refining paleotemperature estimation. *Geochemistry, Geophysics, Geosystems*, *3*(4), 1–29. https://doi.org/10.1029/2001gc000200

Delaney, M. L., Be, A. W. H., & Boyle, E. A. (1985). Li, Sr, Mg, and Na in foraminiferal calcite shells from laboratory culture, sediment traps, and sediment cores. *Geochimica et Cosmochimica Acta*, *49*, 1327–1341. https://doi.org/10.1016/0016-7037(85)90284-4

Dickson, J. (2002). Fossil echinoderms as monitor of the Mg/Ca ratio of Phanerozoic oceans. *Science*, *298*(5596), 1222–1224. https://doi.org/10.1126/science.1075882

Dickson, J. (2004). Echinoderm skeletal preservation: Calcite-aragonite seas and the Mg/Ca ratio of Phanerozoic oceans. *Journal of Sedimentary Research*, *74*(3), 355–365. https://doi.org/10.1306/112203740355

Drury, A. J., Lee, G. P., Gray, W. R., Lyle, M., Westerhold, T., Shevenell, A. E., & John, C. M. (2018). Deciphering the state of the late Miocene to early Pliocene equatorial Pacific. *Paleoceanography and Paleoclimatology*, *33*(3), 246–263. https://doi.org/10.1002/2017pa003245

Elderfield, H., Vautravers, M., & Cooper, M. (2002). The relationship between shell size and Mg/Ca, Sr/Ca, δ18O, and δ13C of species of planktonic foraminifera. *Geochemistry, Geophysics, Geosystems*, *3*(8), 1–13. https://doi.org/10.1029/2001gc000194

Elderfield, H., Yu, J., Anand, P., Kiefer, T., & Nyland, B. (2006). Calibrations for benthic foraminiferal Mg/Ca paleothermometry and the carbonate ion hypothesis. *Earth and Planetary Science Letters*, *250*(3), 633–649. https://doi.org/10.1016/j.epsl.2006.07.041

Evans, D., & Mueller, W. (2012). Deep time foraminifera Mg/Ca paleothermometry: Nonlinear correction for secular change in seawater Mg/Ca. *Paleoceanography*, *27*(4). https://doi.org/10.1029/2012pa002315

Evans, D., Wade, B. S., Henehan, M., Erez, J., & Müller, W. (2016). Revisiting carbonate chemistry controls on planktic foraminifera Mg/Ca: Implications for sea surface temperature and hydrology shifts over the Paleocene-wecene thermal maximum and eocene-oligocene transition. *Climate of the Past*, *12*, 819–835. https://doi.org/10.5194/cp-12-819-2016

Fairbanks, R. G., Sverdlove, M., Free, R., Wiebe, P. H., & Bé, A. W. (1982). Vertical distribution and isotopic fractionation of living planktonic foraminifera from the Panama Basin. *Nature*, *298*(5877), 841–844. https://doi.org/10.1038/298841a0

Fantle, M. S., & DePaolo, D. J. (2005). Variations in the marine Ca cycle over the past 20 million years. *Earth and Planetary Science Letters*, *237*(1), 102–117. https://doi.org/10.1016/j.epsl.2005.06.024

Fantle, M. S., & DePaolo, D. J. (2006). Sr isotopes and pore fluid chemistry in carbonate sediment of the Ontong Java Plateau: Calcite recrystallization rates and evidence for a rapid rise in seawater Mg over the last 10 million years. *Geochimica et Cosmochimica Acta*, *70*(15), 3883–3904. https://doi.org/10.1016/j.gca.2006.06.009

Fedorov, A. V., Burls, N. J., Lawrence, K. T., & Peterson, L. C. (2015). Tightly linked zonal and meridional sea surface temperature gradients over the past five million years. *Nature Geoscience*, *8*, 975–980. https://doi.org/10.1038/NGEO2577

Fedorov, A. V., Dekens, P. S., McCarthy, M., Ravelo, A. C., deMenocal, P. B., Barreiro, M., et al. (2006). The Pliocene Paradox (Mechanisms for a Permanent El Niño). *Science*, *312*(5779), 1485–1489. https://doi.org/10.1126/science.1122666

Fehrenbacher, J., Martin, P. A., & Eshel, G. (2006). Glacial deep water carbonate chemistry inferred from foraminiferal Mg/Ca: A case study from the western tropical Atlantic. *Geochemistry, Geophysics, Geosystems*, *7*(9). https://doi.org/10.1029/2005GC001156

Fox, L. R., & Wade, B. S. (2013). Systematic taxonomy of Early–Middle Miocene planktonic foraminifera from the equatorial Pacific Ocean: Integrated ocean drilling program, Site U1338. *Journal of Foraminiferal Research*, *43*(4), 374–405. https://doi.org/10.2113/gsjfr.43.4.374

Gasperi, J. T., & Kennett, J. P. (1993). Vertical thermal structure evolution of Miocene surface waters: Western equatorial Pacific DSDP Site 289. *Marine Micropaleontology*, *22*(3), 235–254. https://doi.org/10.1016/0377-8398(93)90046-z

Gray, W. R., & Evans, D. (2019). Nonthermal influences on Mg/Ca in planktonic foraminifera: A review of culture studies and application to the Last Glacial Maximum. *Paleoceanography and Paleoclimatology*, *34*, 306–315. https://doi.org/10.1029/2018pa003517

Herold, N., Huber, M., Müller, R. D., & Seton, M. (2012). Modeling the Miocene climatic optimum: Ocean circulation. *Paleoceanography*, *27*(1), PA1209. https://doi.org/10.1029/2010pa002041

Holbourn, A., Kuhnt, W., Frank, M., & Haley, B. (2013). Changes in Pacific Ocean circulation following the Miocene onset of permanent Antarctic ice cover. *Earth and Planetary Science Letters*, *365*, 38–50. https://doi.org/10.1016/j.epsl.2013.01.020

Holbourn, A., Kuhnt, W., Lyle, M., Schneider, L., Romero, O., & Andersen, N. (2014). Middle Miocene climate cooling linked to intensification of eastern equatorial Pacific upwelling. *Geology*, *42*(1), 19–22. https://doi.org/10.1130/g34890.1

Holbourn, A., Kuhnt, W., Regenberg, M., Schulz, M., Mix, A., & Andersen, N. (2010). Does Antarctic glaciation force migration of the tropical rain belt? *Geology*, *38*(9), 783–786. https://doi.org/10.1130/g31043.1

Holbourn, A., Kuhnt, W., Schulz, M., Flores, J.-A., & Andersen, N. (2007). Orbitally-paced climate evolution during the middle Miocene "Monterey" carbon-isotope excursion. *Earth and Planetary Science Letters*, *261*(3), 534–550. https://doi.org/10.1016/j.epsl.2007.07.026

Horita, J., Zimmermann, H., & Holland, H. D. (2002). Chemical evolution of seawater during the Phanerozoic: Implications from the record of marine evaporates. *Geochimica et Cosmochimica Acta*, *66*(21), 3733–3756. https://doi.org/10.1016/s0016-7037(01)00884-5

Karnauskas, K. B., Seager, R., Kaplan, A., Kushnir, Y., & Cane, M. A. (2009). Observed strengthening of the zonal sea surface temperature gradient across the equatorial Pacific Ocean. *Journal of Climate*, *22*(16), 4316–4321. https://doi.org/10.1175/2009jcli2936.1

Kennett, J. P., Keller, G., & Srinivasan, M. (1985). Miocene planktonic foraminiferal biogeography and paleoceanographic development of the Indo-Pacific region. *Geological Society of America Memoirs*, *163*, 197–236. https://doi.org/10.1130/mem163-p197

Kennett, J. P., & Srinivasan, M. S. (1983). *Neogene planktonic foraminifera: A phylogenetic atlas*. Stroudsburg, PA: Hutchinson Ross Publishing Co.

Kim, S. T., & O'Neil, J. R. (1997). Equilibrium and nonequilibrium oxygen isotope effects in synthetic carbonates. *Geochimica et Cosmochimica Acta*, *61*(16), 3461–3475. https://doi.org/10.1016/s0016-7037(97)00169-5

Kochhann, K. G. D., Holbourn, A., Kuhnt, W., Channell, J. E. T., Lyle, M., Shackford, J. K., et al. (2016). Eccentricity pacing of eastern equatorial Pacific carbonate dissolution cycles during the Miocene Climatic Optimum. *Paleoceanography*, *31*(9), 1176–1192. https://doi.org/10.1002/2016pa002988

Koutavas, A., & Lynch-Stieglitz, J. (2004). Variability of the marine ITCZ over the eastern Pacific during the past 30,000 years. In: *The Hadley circulation: Present, past and future* (pp. 347–369). Dordrecht: Springer. https://doi.org/10.1007/978-1-4020-2944-8_13

Lea, D. W., Pak, D. K., & Spero, H. J. (2000). Climate impact of late quaternary equatorial Pacific Sea surface temperature variations. *Science*, *289*(5485), 1719–1724. https://doi.org/10.1126/science.289.5485.1719

Lear, C. H., Bailey, T. R., Pearson, P. N., Coxall, H. K., & Rosenthal, Y. (2008). Cooling and ice growth across the eocene-oligocene transition. *Geology*, *36*(3), 251–254.

Lin, C.-Y., Zheng, Q., Ho, C.-R., Huang, S.-J., & Kuo, N.-J. (2011). Variability of sea surface temperature and warm pool area in the South China Sea and its relationship to the western Pacific warm pool. *Journal of Oceanography*, *67*, 719–724. https://doi.org/10.1007/s10872-011-0072-x

Liu, J., Tian, J., Liu, Z., Herbert, T. D., Fedorov, A. V., & Lyle, M. (2019). Eastern equatorial Pacific cold tongue evolution since the late Miocene linked to extratropical climate. *Science advances*, *5*(4), eaau6060. https://doi.org/10.1126/sciadv.aau6060

Lowenstein, T. K., Timofeeff, M. N., Brennan, S. T., Hardie, L. A., & Demicco, R. (2001). Oscillations in Phanerozoic seawater chemistry: Evidence from fluid inclusions. *Science*, *294*(5544), 1086–1088. https://doi.org/10.1126/science.1064280

Lyle, M., Wilson, P., & Janacek, T. (2002). Leg 199. In: *Proceedings of the Ocean Drilling Program* (pp. 1–87). Initial Reports, 199

Martin, P. A., & Lea, D. W. (2002). A simple evaluation of cleaning procedures on fossil benthic foraminiferal Mg/Ca. *Geochemistry, Geophysics, Geosystems*, *3*(10), 1–8. https://doi.org/10.1029/2001gc000280

Martínez-Garcia, A., Rosell-Melé, A., McClymont, E. L., Gersonde, R., & Haug, G. H. (2010). Subpolar link to the emergence of the modern equatorial Pacific cold tongue. *Science*, *328*(5985), 1550–1553.

Martins, S. M., & Stammer, D. (2015). Pacific Ocean surface freshwater variability underneath the double ITCZ as seen by satellite sea surface salinity retrievals. *Journal of Geophysical Research: Oceans*, *120*, 5870–5885. https://doi.org/10.1002/2015JC010895

Matsui, H., Nishi, H., Kuroyanagi, A., Hayashi, H., Ikehara, M., & Takashima, R. (2017). Vertical thermal gradient history in the eastern equatorial Pacific during the early to middle Miocene: Implications for the equatorial thermocline development. *Paleoceanography*, *32*(7), 729–743. https://doi.org/10.1002/2016pa003058

McGee, D., Donohoe, A., Marshall, J., & Ferreira, D. (2014). Changes in ITCZ location and cross-equatorial heat transport at the Last Glacial Maximum, Heinrich Stadial 1, and the mid-Holocene. *Earth and Planetary Science Letters*, *390*, 69–79. https://doi.org/10.1016/j.epsl.2013.12.043

Melnichenko, O., Hacker, P., Bingham, F., Lee, T., & Lee, T. (2019). Patterns of SSS variability in the eastern tropical Pacific: Intraseasonal to interannual timescales from seven years of NASA satellite data. *Oceanography*, *32*(2), 20–29. https://doi.org/10.5670/oceanog.2019.208

Modestou, S. E., Leutert, T., Fernandez, A., Lear, C. H., & Meckler, A. N. (2020). Warm middle Miocene Indian Ocean bottom water temperatures: Comparison of clumped isotope and Mg/Ca based estimates. *Paleoceanography and Paleoclimatology*, *35*. https://doi.org/10.1029/2020PA003927

Moore, T. C., Jr., Backman, J., Raffi, I., Nigrini, C., Sanfilippo, A., Pälike, H., & Lyle, M. (2004). Paleogene tropical Pacific: Clues to circulation, productivity, and plate motion. *Paleoceanography*, *19*(3). https://doi.org/10.1029/2003PA000998

Nathan, S. A., & Leckie, R. M. (2003). Miocene planktonic foraminiferal biostratigraphy of sites 1143 and 1146, ODP Leg 184, South China Sea. *Scientific Results*, *184*, 1–43.

Nathan, S. A., & Leckie, R. M. (2009). Early history of the Western Pacific warm pool during the middle to late Miocene (~ 13.2–5.8 Ma): Role of sea-level change and implications for equatorial circulation. *Paleogeography, Paleoclimatology, Paleoecology*, *274*(3), 140–159. https://doi.org/10.1016/j.palaeo.2009.01.007

O'Brien, C. L., Foster, G. L., Martinez-Boti, M. A., Abell, R., Rae, J. W. B., & Pancost, R. D. (2014). High sea surface temperatures in tropical warm pools during the Pliocene. *Nature Geoscience*, *7*(8), 606–611.

Pälike, H., Lyle, M., Nishi, H., Raffi, I., Gamage, K., & Klaus, A. (2010). *Proc. IODP,* 320/321 & the Expedition 320/321 Scientists. Tokyo: Integrated Ocean Drilling Program Management International, Inc. https://doi.org/10.2204/iodp.proc.320321.2010

Pälike, H., Lyle, M. W., Nishi, H., Raffi, I., Ridgwell, A., Gamage, K., et al. (2012). A Cenozoic record of the equatorial Pacific carbonate compensation depth. *Nature*, *488*(7413), 609–614.

Pearson, P. (1995). Planktonic foraminifer biostratigraphy and the development of pelagic caps on guyots in the Marshall Islands group. *Proceedings of the Ocean Drilling Program: Scientific Results*, *144*, 21–59.

Poole, C. R., & Wade, B. S. (2019). Systematic taxonomy of the *Trilobatus sacculifer* plexus and descendant *Globigerinoidesella fistulosa* (planktonic foraminifera). *Journal of Systematic Palaeontology*, *17*(23), 1989–2030. https://doi.org/10.1080/14772019.2019.1578831

Ravelo, A. C., & Fairbanks, R. G. (1992). Oxygen isotopic composition of multiple species of planktonic foraminifera: Recorders of the modern photic zone temperature gradient. *Paleoceanography*, *7*(6), 815–831.

Regenberg, M., Nürnberg, D., Steph, S., Groeneveld, J., Garbe-Schönberg, D., Tiedemann, R., & Dullo, W. C. (2006). Assessing the effect of dissolution on planktonic foraminiferal Mg/Ca ratios: Evidence from Caribbean core tops. *Geochemistry, Geophysics, Geosystems*, *7*(7). https://doi.org/10.1029/2005gc001019

Riser, S. C., Yang, J., Drucker, R., & Drucker, R. (2019). Observations of large-scale rainfall, wind, and sea surface salinity variability in the eastern tropical Pacific. *Oceanography*, *32*(2), 42–49. https://doi.org/10.5670/oceanog.2019.211

Rosenthal, Y., Lear, C. H., Oppo, D. W., & Linsley, B. K. (2006). Temperature and carbonate ion effects on Mg/Ca and Sr/Ca ratios in benthic foraminifera: Aragonitic species *Hoeglundina elegans*. *Paleoceanography*, *21*(1), PA1007. https://doi.org/10.1029/2005pa001158

Rosenthal, Y., Perron-Cashman, S., Lear, C. H., Bard, E., Barker, S., Billups, K., et al. (2004). Interlaboratory comparison study of Mg/Ca and Sr/Ca measurements in planktonic foraminifera for paleoceanographic research. *Geochemistry, Geophysics, Geosystems*, *5*(4).

Rousselle, G., Beltran, C., Sicre, M.-A., Raffi, I., & De Rafelis, M. (2013). Changes in sea-surface conditions in the Equatorial Pacific during the middle Miocene–Pliocene as inferred from coccolith geochemistry. *Earth and Planetary Science Letters*, *361*, 412–421. https://doi.org/10.1016/j.epsl.2012.11.003

Shevenell, A. E., Kennett, J. P., & Lea, D. W. (2004). Middle Miocene southern ocean cooling and Antarctic cryosphere expansion. *Science*, *305*(5691), 1766–1770. https://doi.org/10.1126/science.1100061

Shevenell, A. E., Kennett, J. P., & Lea, D. W. (2008). Middle Miocene ice sheet dynamics, deep-sea temperatures, and carbon cycling: A Southern Ocean perspective. *Geochemistry, Geophysics, Geosystems*, *9*(2). https://doi.org/10.1029/2007GC001736

Sime, N. G., Christina, L., Tipper, E. T., Tripati, A., Galy, A., & Bickle, M. J. (2007). Interpreting the Ca isotope record of marine biogenic carbonates. *Geochimica et Cosmochimica Acta*, *71*(16), 3979–3989. https://doi.org/10.1016/j.gca.2007.06.009

Sosdian, S. M., Babila, T. L., Greenop, R., Foster, G. L., & Lear, C. H. (2020). Ocean carbon storage across the middle Miocene: A new interpretation for the monterey event. *Nature Communications*, *11*(1), 1–11. https://doi.org/10.1038/s41467-019-13792-0

Sosdian, S. M., & Lear, C. H. (2020). Initiation of the Western Pacific Warm Pool at the Middle Miocene Climate Transition? *Paleoceanography and Paleoclimatology*, *32*, e2020PA003920. https://doi.org/10.1029/2020PA003920

Spezzaferri, S., Olsson, R. K., & Hemleben, C. (2018). Taxonomy, biostratigraphy, and phylogeny of Oligocene to lower Miocene *Globigerinoides* and *Trilobatus*. *Cushman Found*, *46*, 269–306.

Stanley, S. M., & Hardie, L. A. (1999). Hypercalcification: Paleontology links plate tectonics and geochemistry to sedimentology. *GSA today*, *9*(2), 1–7.

Steph, S., Regenberg, M., Tiedemann, R., Mulitza, S., & Nürnberg, D. (2009). Stable isotopes of planktonic foraminifera from tropical Atlantic/Caribbean core-tops: Implications for reconstructing upper ocean stratification. *Marine Micropaleontology*, *71*(1–2), 1–19.

Steph, S., Tiedemann, R., Prange, M., Groeneveld, J., Schulz, M., Timmermann, A., et al. (2010). Early Pliocene increase in thermohaline overturning: A precondition for the development of the modern equatorial Pacific cold tongue. *Paleoceanography*, *25*, PA2202. https://doi.org/10.1029/2008pa001645

Stott, L., Cannariato, K., Thunell, R., Haug, G. H., Koutavas, A., & Lund, S. (2004). Decline of surface temperature and salinity in the western tropical Pacific Ocean in the Holocene epoch. *Nature*, *431*(7004), 56–59. https://doi.org/10.1038/nature02903

Tian, J., Yang, M., Lyle, M. W., Wilkens, R., & Shackford, J. K. (2013). Obliquity and long eccentricity pacing of the Middle Miocene climate transition. *Geochemistry, Geophysics, Geosystems*, *14*(6), 1740–1755. https://doi.org/10.1002/ggge.20108

Tierney, J. E., Malevich, S. B., Gray, W., Vetter, L., & Thirumalai, K. (2019). Bayesian calibration of the Mg/Ca paleothermometer in planktic foraminifera. *Paleoceanography and Paleoclimatology*, *34*(12), 2005–2030. https://doi.org/10.1029/2019pa003744

Tyberghein, L., Verbruggen, H., Pauly, K., Troupin, C., Mineur, F., & De Clerck, O. (2012). Bio-ORACLE: A global environmental dataset for marine species distribution modelling. *Global Ecology and Biogeography*, *21*, 272–281. https://doi.org/10.1111/j.1466-8238.2011.00656.x

Wade, B. S., Houben, A. J. P., Quaijtaal, W., Schouten, S., Rosenthal, Y., Miller, K. G., et al. (2012). Multiproxy record of abrupt sea surface cooling across the Eocene-Oligocene transition in the Gulf of Mexico. *Geology*, *40*(2), 159–162. https://doi.org/10.1130/g32577.1

Wade, B. S., O'Neill, J. F., Phujareanchaiwon, C., Ali, I., Lyle, M., Witkowski, J., & Witkowski, J. (2020). Evolution of deep-sea sediments across the Paleocene-Eocene and Eocene-Oligocene boundaries. *Earth-Science Reviews*, *211*, 103403. https://doi.org/10.1016/j.earscirev.2020.103403

Wade, B. S., Pearson, P. N., Berggren, W. A., & Pälike, H. (2011). Review and revision of Cenozoic tropical planktonic foraminiferal biostratigraphy and calibration to the geomagnetic polarity and astronomical time scale. *Earth-Science Reviews*, *104*, 111–142.

Wara, M. W., Ravelo, A. C., & Delaney, M. L. (2005). Permanent El Niño-Like conditions during the Pliocene Warm Period. *Science*, *309*(5735), 758–761. https://doi.org/10.1126/science.1112596

Westerhold, T., Bickert, T., & Röhl, U. (2005). Middle to late Miocene oxygen isotope stratigraphy of ODP site 1085 (SE Atlantic): New constraints on Miocene climate variability and sea-level fluctuations. *Paleogeography, Paleoclimatology, Paleoecology*, *217*(3), 205–222. https://doi.org/10.1016/j.palaeo.2004.12.001

Wyrtki, K. (1981). An estimate of equatorial upwelling in the Pacific. *Journal of Physical Oceanography*, *11*(9), 1205–1214. https://doi.org/10.1175/1520-0485(1981)011<1205:aeoeui>2.0.co;2

Yan, X. H., Ho, C. R., Zheng, Q., & Klemas, V. (1992). Temperature and size variabilities of the Western Pacific Warm Pool. *Science*, *258*(5088), 1643–1645. https://doi.org/10.1126/science.258.5088.1643

Yang, H., Lohmann, G., Lu, J., Gowan, E. J., Shi, X., Liu, J., & Wang, Q. (2020). Tropical expansion driven by poleward advancing midlatitude meridional temperature gradients. *Journal of Geophysical Research: Atmospheres*, *125*, e2020JD033158. https://doi.org/10.1029/2020JD033158

Zhang, Y. G., Pagani, M., Henderiks, J., & Ren, H. (2017). A long history of equatorial deep-water upwelling in the Pacific Ocean. *Earth and Planetary Science Letters*, *467*, 1–9.

Zhang, Y. G., Pagani, M., & Liu, Z. (2014). A 12-million-year temperature history of the tropical pacific ocean. *Science*, *344*(6179), 84–87. https://doi.org/10.1126/science.1246172

Zheng, Y., Lin, J. L., & Shinoda, T. (2012). The equatorial Pacific cold tongue simulated by IPCC AR4 coupled GCMs: Upper ocean heat budget and feedback analysis. *Journal of Geophysical Research*, *117*(C5). https://doi.org/10.1029/2011jc007746